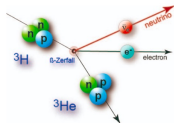
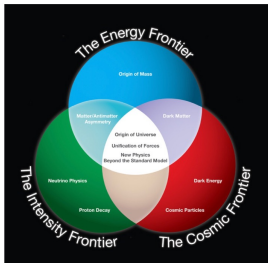


Modeling $0\nu\beta\beta$ decay based on nuclear forces and transition operators from chiral effective field theory

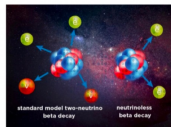
Jiangming Yao (尧江明)

School of Physics and Astronomy, Sun Yat-sen University
中山大学物理与天文学院

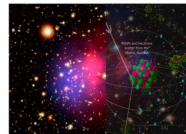
第九届手征有效场论研讨会
2024年10月19日，中国长沙



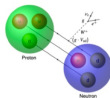
Single-beta decay



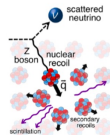
Neutrinoless double beta decay



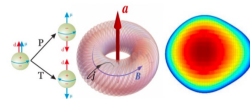
Dark matter direct detection



Superallowed Fermi transitions



Neutrino scattering



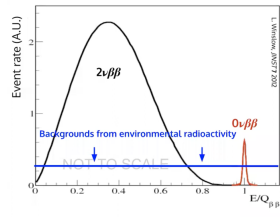
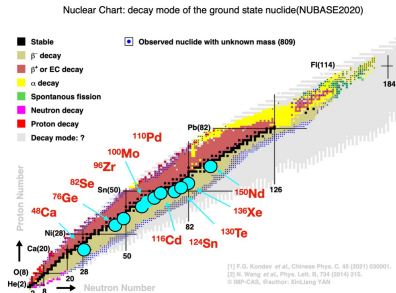
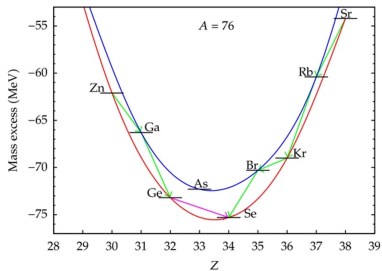
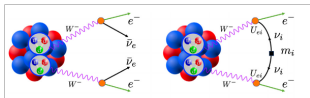
Symmetry-violating moments

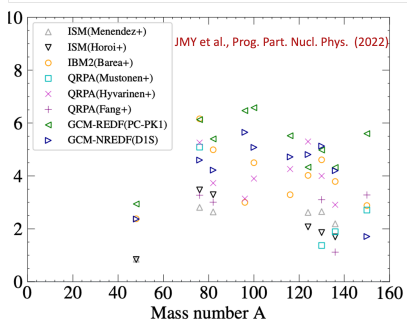
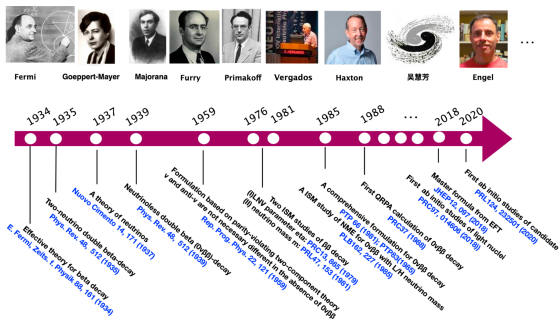
- **High-intensity frontiers:** searching for $0\nu\beta\beta$ decay, dark matter detector, atomic EDM, etc.
- **Accurate nuclear matrix elements:** crucial for testing fundamental symmetries and interactions with low-energy probes.

A hypothetical nuclear decay mode: $0\nu\beta\beta$ decay

- The two modes of $\beta^-\beta^-$ decay:

$$(A, Z) \rightarrow (A, Z + 2) + 2e^- + (2\bar{\nu}_e)$$

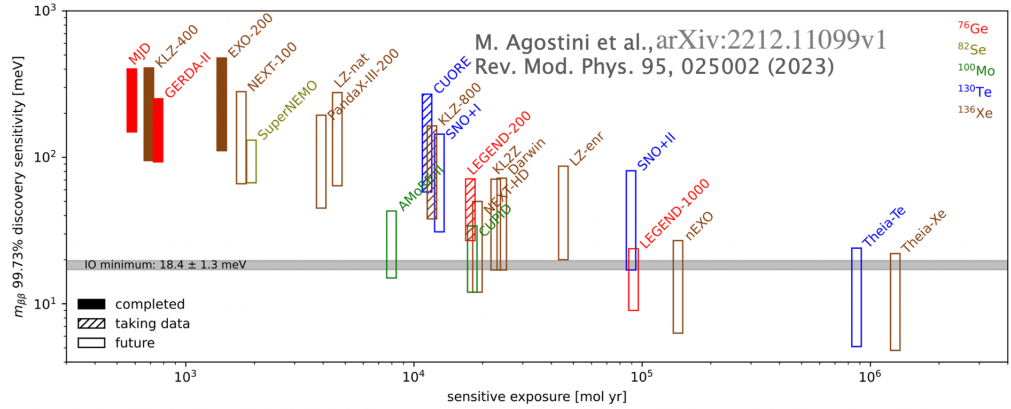




If $0\nu\beta\beta$ decay is driven by exchanging light massive Majorana neutrinos,

$$\langle m_{\beta\beta} \rangle \equiv \left| \sum_{j=1}^3 U_{ej}^2 m_j \right| = \left[\frac{m_e^2}{g_A^4 G_{0\nu} T_{1/2}^{0\nu} |M^{0\nu}|^2} \right]^{1/2}$$

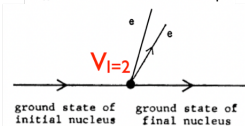
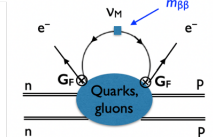
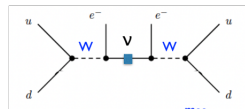
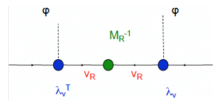
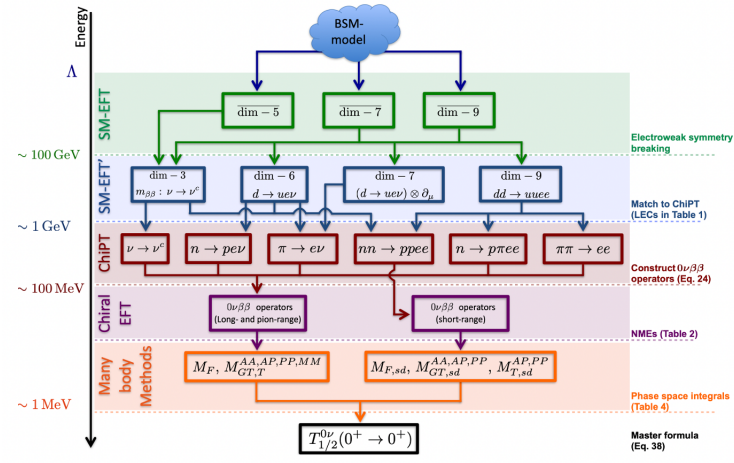
Accurate values of the NMEs $M^{0\nu}$ are crucial for designing and interpreting those experiments, as they link the observed decay rate to the neutrino mass scale.

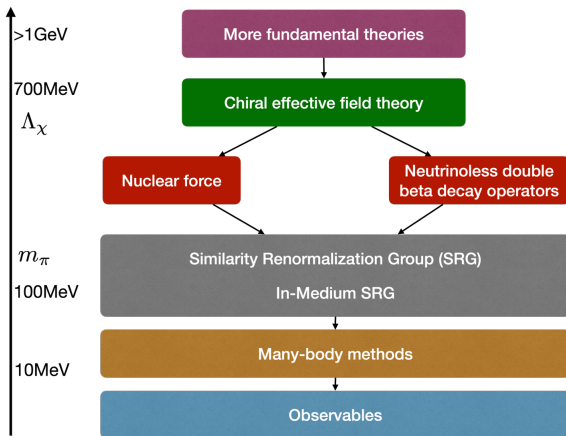


- Lifetime sensitivity of the ton-scale experiments: $T_{1/2}^{0\nu} > 10^{28}$ yr.
- Whether or not the ton-scale experiments are able to cover the entire parameter space for the IO case depends strongly on the employed NME.

The EFT provides a model-independent framework for describing $0\nu\beta\beta$ decay.

Cirigliano (2018)



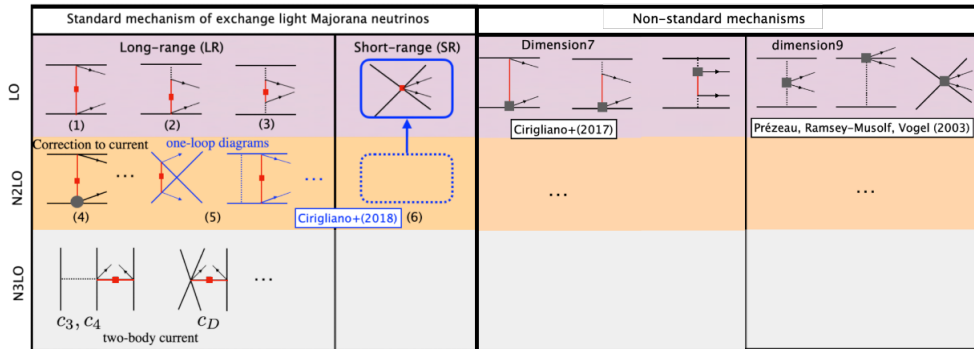


The basic idea of current efforts:

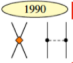



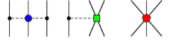
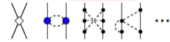
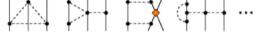
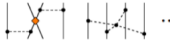
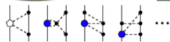


- Identify the active dof at the nuclear energy scale: $N, \pi, (e, \nu)$
- Write down all possible contributions to both nuclear force and transition operators according to a power counting rule, $(Q, m_\pi)/\Lambda_\chi$.
- Carry out a quantum many-body calculation and compute the NME.

- At $E \sim 100$ MeV: operators are expressed in terms of nucleons, pions, and leptons, arranged in the order $(Q, m_\pi/\Lambda_\chi)^\nu$,

$$\nu = 2A + 2L - 2 + \sum_i \left(\frac{n_f}{2} + d - 2 + n_e \right)_i$$



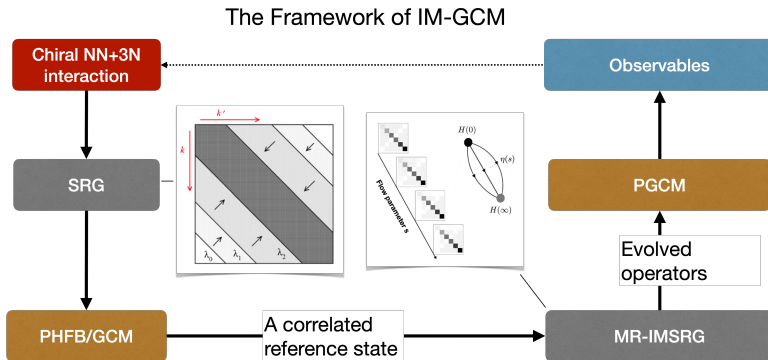
- Non-relativistic chiral 2N+3N interactions (Weinberg power counting and others)

	NN	3N	4N
LO $\alpha(Q^0/\Lambda^0)$	 1990 Weinberg 2	—	—
NLO $\alpha(Q^2/\Lambda^2)$	 1992 Ordonez, van Kolck 7	 1992,1994 [166-169]	—
N ² LO $\alpha(Q^3/\Lambda^3)$	 1992 Ordonez, van Kolck 0	 1994 Weinberg van Kolck Epelbaum 2	—
N ³ LO $\alpha(Q^4/\Lambda^4)$	 2000–2002 Kaiser 12	 2008–2011 [183-185] 0	 2006 [186] 0
N ⁴ LO $\alpha(Q^5/\Lambda^5)$	 2015 [188,189] 0	 2011– [190-192] ?	 ?

K. Hebeler, Phys. Rep. 890, 1 (2020)

- Relativistic chiral 2N interaction (up to N²LO, different PC from the NR case)

J.-X. Lu et al., PRL128, 142002 (2022)



- **In-medium similarity renormalization group (IMSRG)**: capture dynamic correlations associated with high-energy few-particle, few-hole excitations
- **Projected generator coordinate method (PGCM)**: include the collective (static) correlations associated with pairing and deformation.

- Multi-reference in-medium generator coordinate method (IM-GCM)

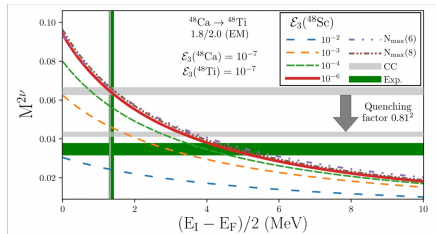
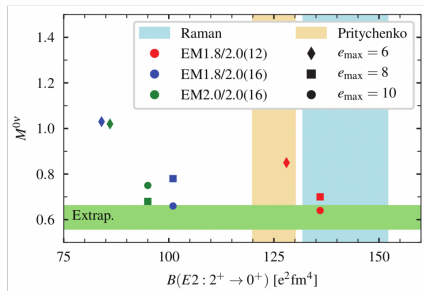
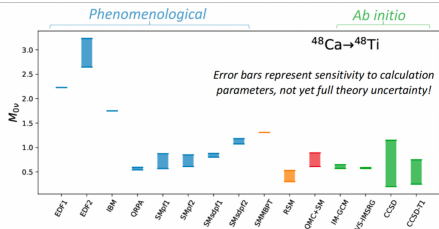
JMY et al., PRL124, 232501 (2020)

- Valence-space shell model+IMSRG (VS-IMSRG)

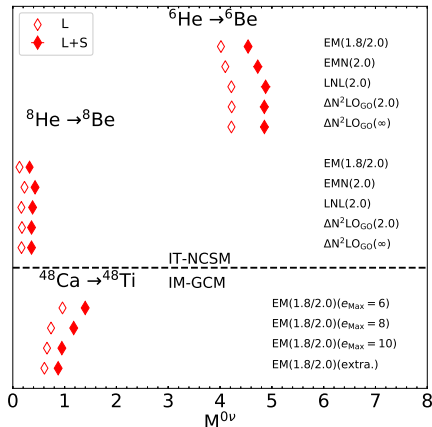
A. Belley et al., PRL126, 042502 (2021)

- Coupled-cluster with singlets, doublets, and partial triplets (CCSDT1)

S. Novario et al., PRL126, 182502 (2021)



- The contact transition operator could either enhance or quench the $0\nu\beta\beta$ decay of candidate nuclei.
- The LEC g_ν^{NN} consistent with the employed chiral interaction (EM1.8/2.0) is determined based on the synthetic data.
- The contact term turns out to enhance the NME for ^{48}Ca by 43(7)%, thus reducing the half-life $T_{1/2}^{0\nu}$ significantly.



R. Wirth, JMY, H. Hergert, PRL127, 242502 (2021)

The true value of the NME can be written as

$$M^{0\nu} = M_k^{0\nu} + \epsilon_{\chi\text{EFT}} + \epsilon_{\text{MBT}} + \epsilon_{\text{OP}} + \epsilon_{\text{EM}},$$

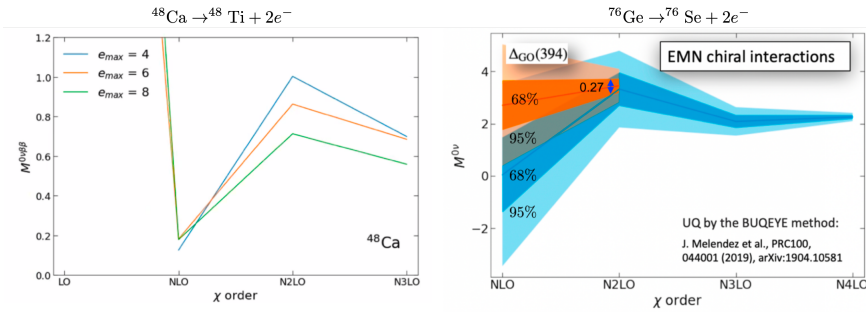
where the posterior probability distribution (PPD) of an LEC sample to yield results for a set of calibration observables that match experimental data

$$\text{PPD} = \{M_k^{0\nu}(\mathbf{c}) : \mathbf{c} \sim \mathcal{P}(\mathbf{c}|\text{calibration})\}.$$

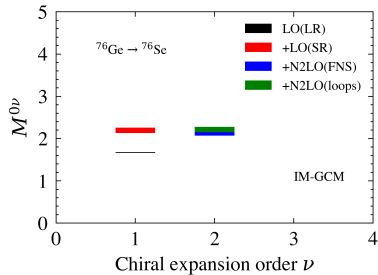
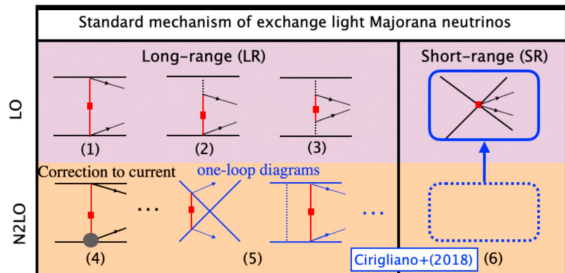
from which one finds the statistical error χ_{LEC} ,

- $\epsilon_{\chi\text{EFT}}$: chiral expansion truncation on nuclear forces
- ϵ_{MBT} : approximation in many-body methods
- ϵ_{OP} : chiral expansion truncation on transition operators
- ϵ_{EM} : the error of the emulator

All the errors ϵ are assumed to be normally distributed and mutually independent.



- The NME converges with respect to the chiral expansion order χ of nuclear forces for candidate nuclei ^{48}Ca and ^{76}Ge .
- The EFT truncation error (evaluated using the BUQEYE method) is shrinking with χ .



- In the N2LO, we choose $\mu_{US} = m_\pi$ to eliminate all the terms depending on $\ln \frac{m_\pi^2}{\mu_{US}^2}$, and the LECs of the counterterms as $g_\nu^{\pi\pi} = -7.6 - (36/5) \ln(\mu/m_\rho)$, and $g_\nu^{\pi N} = 0$. V. Cirigliano, et al., PRC97, 065501 (2018)
- The NME for ^{76}Ge converges with respect to the chiral expansion order of transition operators.

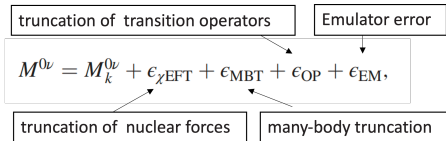
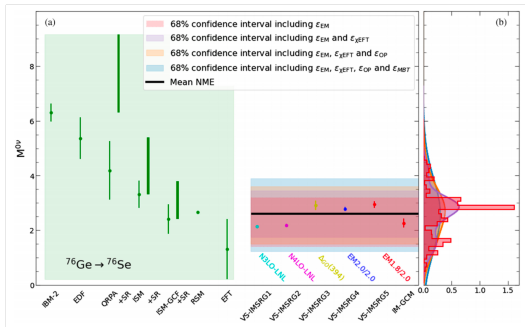


TABLE I. The recommended value for the total NME of $0\nu\beta\beta$ decay in ^{76}Ge , together with the uncertainties from different sources.

$M^{0\nu}$	ϵ_{LEC}	$\epsilon_{\chi\text{EFT}}$	ϵ_{MBT}	ϵ_{OP}	ϵ_{EM}
$2.60^{+1.28}_{-1.36}$	0.75	0.3	0.88	0.47	< 0.06



- Our recommended value $M^{0\nu} = 2.60^{+1.28}_{-1.36}$.
- Together with the best half-life limit: $> 1.8 \times 10^{26}$ yr, it sets the upper limit $\langle m_{\beta\beta} \rangle = 187^{+205}_{-62}$ meV, and the sensitivity of the next-generation experiment $\langle m_{\beta\beta} \rangle = 22^{+24}_{-7}$ meV, covering almost the entire range of IO hierarchy.

- $0\nu\beta\beta$ decay: only way to determine the nature of neutrinos, a complementary way to determine the absolute mass scale of neutrinos. **The NMEs of candidate nuclei are crucial for designing and interpreting those experiments.**
- **Large uncertainty in NMEs:** major systematical uncertainty, impacting the interpretation of the measurements.
- **Remarkable progress in ab initio studies of NMEs:** development of a novel ab initio method for candidate nuclei, disclosing non-trivial contributions from high-energy light neutrinos, and rapid convergence w.r.t. the chiral expansion order, a comprehensive uncertainty quantification.

What's next?

- The NMEs of heavier candidates ^{82}Se , ^{100}Mo , ^{130}Te , ^{136}Xe , with reduced uncertainty by considering higher-order nuclear interactions, reducing many-body truncation errors, and finding more constraints to shrink the uncertainty.
- Contributions from **non-standard mechanisms**.

Collaborators

- **SYSU**

C.R. Ding, Q.Y. Luo, C.F. Jiao, C.C. Wang, G. Li, X. Zhang, E.F. Zhou

- **PKU**

L. S. Song, J. Meng, P. Ring, Y. K. Wang, P. W. Zhao

- **LZU**: Y.F. Niu

- **CAEP**: B.N. Lv

- **SWU**: L.J. Wang

- **MSU**: S. Bogner, H. Hergert, R. Wirth

- **UNC**: J. Engel, A. M. Romero

- **TRIUMF**: A. Belly, J. Holt

- **TU Darmstadt**: T. Miyagi

- **Notre-Dame U**: R. Stroberg

- **UAM**: B. Bally, T. Rodriguez

This work is supported in part by the National Natural Science Foundation of China (Grant Nos. 12141501 and 12275369), the Guangdong Basic and Applied Basic Research Foundation (2023A1515010936).

Thank you for your attention!

- Leading order (LO) A. Belley, JMY et al., PRL132, 182502 (2024)

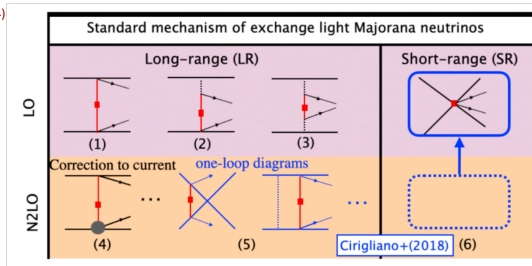
$$O_{\alpha,L}^{\text{LO}}(r_{12}) = \frac{2R}{\pi g_A^2(0)} \int_0^\infty dq q^2 \frac{h_{\alpha,L}^{\text{LO}}(q^2)}{q(q+E_d)} j_L(qr_{12}),$$

$$O_{\text{LO,SR}}^{0\nu} = -2g_V^{NN} \left(\frac{m_N g_A^2}{4f_\pi^2} \right) f_\Lambda^{\text{exp}}(r_{12}) f_\Lambda^{\text{exp}}(r'_{12})$$

$$h_{\text{E},0}^{\text{LO}}(q^2) = -g_V^2(0),$$

$$h_{\text{GT},0}^{\text{LO}}(q^2) = g_A^2(0) - \frac{2}{3} \frac{q^2}{2m_p} g_A(0) g_P(0) + \frac{1}{3} \frac{q^4}{4m_p^2} g_P^2(0),$$

$$h_{\text{T},2}^{\text{LO}}(q^2) = \frac{2}{3} \frac{q^2}{2m_p} g_A(0) g_P(0) - \frac{1}{3} \frac{q^4}{4m_p^2} g_P^2(0).$$



- N2LO

correction to current and induced weak-magnetism

$$g_V(q^2) = g_V(0) \left(1 + q^2/\Lambda_V^2 \right)^{-2},$$

$$g_A(q^2) = g_A(0) \left(1 + q^2/\Lambda_A^2 \right)^{-2}.$$

$$h_{\text{GT},0}^{\text{N2LO}}(q^2) = g_M^2(q^2) \frac{1}{6} \frac{q^2}{m_p^2},$$

$$h_{\text{T},2}^{\text{N2LO}}(q^2) = g_M^2(q^2) \frac{1}{12} \frac{q^2}{m_p^2},$$

loop diagrams

$$O_{\text{N2LO,GT}}^{0\nu} = \frac{4R}{3\pi m_\pi^2 T^2} \int q^4 dq j_0(qr) \left(K_{VV}(\vec{q}) - K_{AA}(\vec{q}) \right) - \frac{2g_A^2 m_\pi^2}{q^2 + m_\pi^2} \ln \frac{m_\pi^2}{\mu_{us}^2} - K_{CT}(\vec{q}) \sigma_1 \cdot \sigma_2,$$

$$O_{\text{N2LO,F}}^{0\nu} = \frac{4R}{\pi T^2} \int q^2 dq j_0(qr) \left(\left[\frac{3C_T T^2}{\pi^2} - \frac{2g_A^2 q^2}{q^2 + m_\pi^2} \right] \ln \frac{m_\pi^2}{\mu_{us}^2} - K'_{AA}(\vec{q}) \right) \mathbf{1}_1 \times \mathbf{1}_2,$$

$$O_{\text{N2LO,T}}^{0\nu} = -\frac{4R}{3m_\pi^2 \pi T^2} \int q^4 dq j_2(qr) \left(K_{VV}(\vec{q}) - K_{AA}(\vec{q}) \right) - \frac{2g_A^2 m_\pi^2}{q^2 + m_\pi^2} \ln \frac{m_\pi^2}{\mu_{us}^2} - K_{CT}(\vec{q}) S'_{12}(\vec{r}),$$

with $\vec{q} = q^2/m_\pi^2$, $T = 4\pi f_\pi$, and $L_\pi = \ln \frac{\mu_\pi^2}{m_\pi^2}$,

$$K_{VV}(\vec{q}) = \frac{2(1-\vec{q})^2}{\vec{q}^2(1+\vec{q})} \ln(1+\vec{q}) - \frac{2}{\vec{q}} + \frac{7-3\vec{q}L_\pi}{(1+\vec{q})^2} + \frac{L_\pi}{1+\vec{q}}$$

$$K_{AA}(\vec{q}) = \frac{g_A^2}{1+\vec{q}} (L_\pi - 4) + \frac{1}{(1+\vec{q})^2},$$

$$K'_{AA}(\vec{q}) = \frac{1}{g_A^2} \left[-\frac{3}{4} (1-g_A^2)^2 L_\pi + g_A^4 f_4(\vec{q}) + g_A^2 f_2(\vec{q}) + f_0(\vec{q}) + 24g_A^2 f_\pi^2 C_T (L_\pi + 1) \right],$$

$$K_{CT}(\vec{q}) = \frac{5}{6} g_V^{\pi\pi} \frac{\vec{q}}{(1+\vec{q})^2} - g_V^{\pi N} \frac{1}{1+\vec{q}}.$$

A. Belley et al, arXiv:2307.15156 (2023)

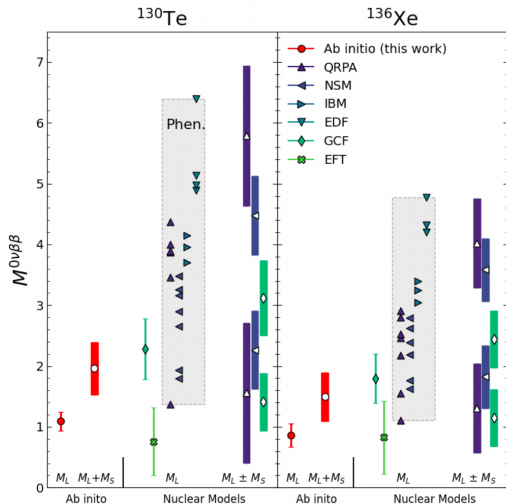
The ab initio VS-IMSRG method is applied to study the NMEs of heavier candidates:

- For ^{130}Te , $M_{L+S}^{0\nu} \in [1.52, 2.40]$
- For ^{136}Xe , $M_{L+S}^{0\nu} \in [1.08, 1.90]$

The uncertainty is composed of different sources: nuclear interaction, reference-state, basis extrapolation, closure approximation, and the LEC for the short-range transition operators.

The values are generally smaller than those from phenomenological nuclear models.

A more comprehensive quantification analysis different nuclear many-body solvers, convergence of NMEs with chiral expansion orders, etc.



- Apply unitary transformations to decouple high and low-momentum states

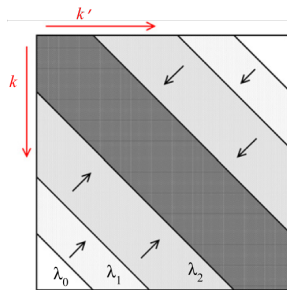
$$H_s = U_s H U_s^\dagger \equiv T_{\text{rel}} + V_s$$

from which one finds the flow equation

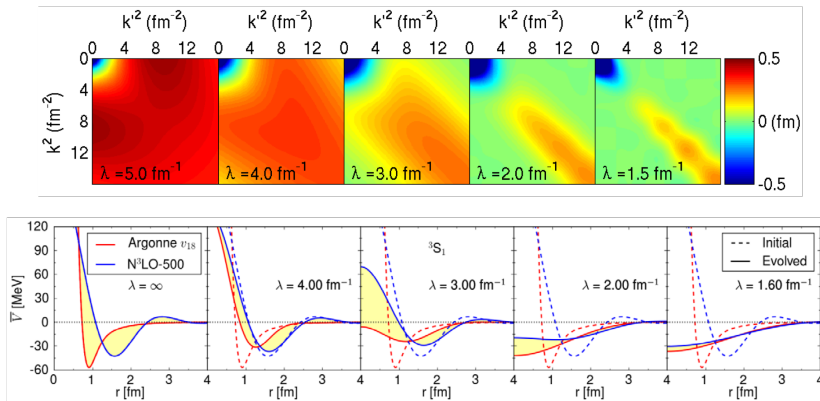
$$\frac{dH_s}{ds} = [\eta_s, H_s], \quad \eta_s = [T_{\text{rel}}, H_s]$$

Evolution of the potential

$$\frac{dV_s(k, k')}{ds} = -(k^2 - k'^2)V_s(k, k') + \frac{2}{\pi} \int_0^\infty q^2 dq (k^2 + k'^2 - 2q^2)V_s(k, q)V_s(q, k')$$



The flow parameter s is usually replaced with $\lambda = s^{-1/4}$ in units of fm^{-1} (a measure of the spread of off-diagonal strength).



- The hard core "disappears" in the SRG softened interactions
- Induced higher-body interactions: $3N, \dots$

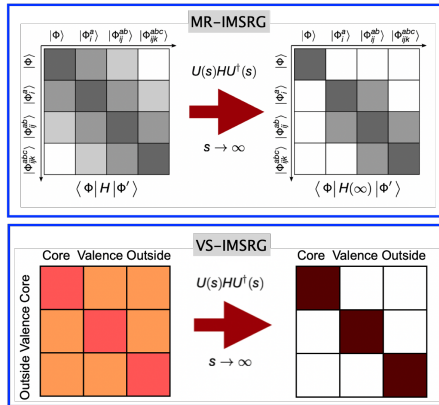
- Apply unitary transformations to H in the configuration space

$$\hat{H}(s) = \hat{U}(s)\hat{H}_0\hat{U}^\dagger(s)$$

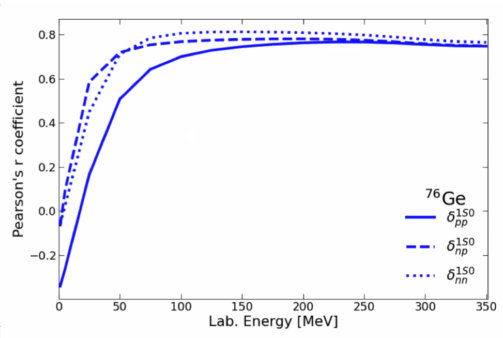
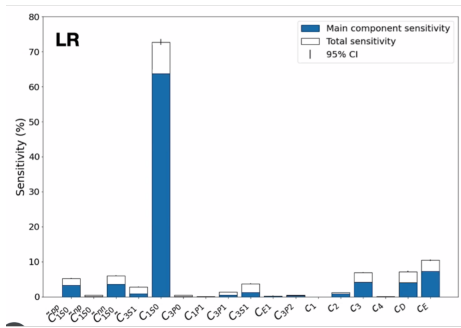
Flow equation

$$\frac{d\hat{H}(s)}{ds} = [\hat{\eta}(s), \hat{H}(s)]$$

- Generator $\eta(s)$: chosen either to decouple a given **reference state** from its excitations or to decouple the valence space from the excluded spaces.
- Not necessary to construct the whole H matrix in the config. space.



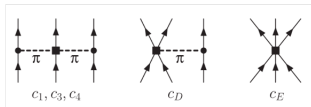
H. Hergert et al., *Phys. Rep.* 621, 165 (2016); S. R. Stroberg et al., *Annu. Rev. Nucl. Part. Sci.* 69, 307 (2019)



- The long-range part of the NME is sensitive to the LEC C_{1S_0} .
- The phase shift of the 1S_0 channel is linearly correlated to the NME.
- The neutron-proton phase-shift $\delta_{np}^{1S_0}$ at 50 MeV is used to weight the samples.

Isotope	$G_{0\nu}$	$M^{0\nu}(\chi\text{EFT})$	$T_{1/2}^{0\nu}$	$\langle m_{\beta\beta} \rangle$	Worldwide Exps current best limits	Inside China
	$[10^{-14} \text{ yr}^{-1}]$	[min, max]	[yr]	[meV]		
76Ge	0.24	$2.60^{+1.27}_{-1.36}$	$> 1.8 \cdot 10^{26}$	187^{+205}_{-62}	GERDA: PRL125, 252502(2020)	CDEX
82Se	1.01		$> 4.6 \cdot 10^{24}$.	CUPID-0: PRL129, 111801 (2023)	NvDEx
^{100}Mo	1.59		$> 3.0 \cdot 10^{24}$		AMoRE: arXiv:2407.05618 [nucl-ex] (2024)	CPUID-China
^{130}Te	1.42	[1.52, 2.40]	$> 2.2 \cdot 10^{25}$	[236, 373]	CUORE: Nature 604, 53(2022)	JUNO
^{136}Xe	1.46	[1.08, 1.90]	$> 2.3 \cdot 10^{26}$	[91, 160]	KamLAND-Zen: PRL130, 051801(2023)	PANDAX

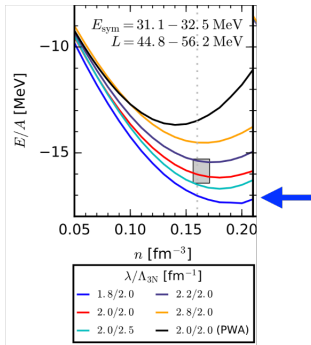
The “magic” interaction EM1.8/2.0: The NN (N³LO: D.R. Entem, R. Machleidt, PRC68 041001 (2003)) and local 3N interactions (N²LO: K. Hebeler et al., PRC83, 031301(R) (2011)).



The LECs of the 3N are fitted on top of the SRG evolved NN interaction.

TABLE I. Results for the c_D and c_E couplings fit to $E_{\text{3H}} = -8.482$ MeV and to the point charge radius $r_{\text{chHe}} = 1.464$ fm (based on Ref. [26]) for the NN/3N cutoffs and different EM/EGM/PWA c_i values used. For $V_{\text{low}k}$ (SRG) interactions, the 3NF fits lead to $E_{\text{3He}} = -28.22 \dots -28.45$ MeV ($-28.53 \dots -28.71$ MeV).

Λ or $\lambda/\Lambda_{\text{3NF}}$ (fm)	$V_{\text{low}k}$		SRG	
	c_D	c_E	c_D	c_E
1.8/2.0 (EM c_i 's)	+1.621	-0.143	+1.264	-0.120
2.0/2.0 (EM c_i 's)	+1.705	-0.109	+1.271	-0.131
2.0/2.5 (EM c_i 's)	+0.230	-0.538	-0.292	-0.592
2.2/2.0 (EM c_i 's)	+1.575	-0.102	+1.214	-0.137
2.8/2.0 (EM c_i 's)	+1.463	-0.029	+1.278	-0.078
2.0/2.0 (EGM c_i 's)	-4.381	-1.126	-4.828	-1.152
2.0/2.0 (PWA c_i 's)	-2.632	-0.677	-3.007	-0.686



C. Drischler et al., PRL122, 042501 (2019)

The saturation properties are not well reproduced.